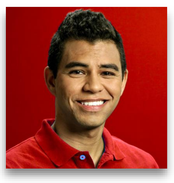

Radiation hydrodynamics of protoplanetary disks with frequency-dependent dust opacities

Stanley A. Baronett[1,2,3], Yan-Fei Jiang (姜燕飞)[1], Philip J. Armitage [1,4], Zhaohuan Zhu (朱照寰)[2,3]

[1] FLATIRON INSTITUTE Center for Computational Astrophysics
[2] NCfA Nevada Center for Astrophysics
[3] UNLV University of Nevada, Las Vegas
[4] Stony Brook University

Introduction

In gaseous protoplanetary disks, sub-micron interstellar dust must grow at least 13 orders of magnitude in size to become terrestrial planets. The frequency-dependent opacities of these silicate grains to pre-main-sequence stellar radiation affect the thermodynamic structure of the disk, which itself influences the various stages of planet formation and migration. With a reduced overall opacity skewed toward shorter wavelengths, the tenuous disk atmosphere heats up as dust preferentially absorbs ultraviolet rays from the young star, while settled grains make the disk midplane optically thick and cooler. Typical disk models, however, often use simplified assumptions about the thermodynamic structure, including vertically-isothermal temperatures and Planck- or Rosseland-mean dust opacities.

Methodology

We use the ATHENA++ hydrodynamics code, extended with multigroup non-relativistic radiation transport (Jiang 2021, 2022), to develop and analyze new stellar-irradiated disk models with frequency-dependent dust opacities. Unlike flux-limited-diffusion or M1 methods for radiation hydrodynamics, the ATHENA++ module solves the time-dependent radiation transport equation,

$$\frac{\partial I_f}{\partial t} + c\mathbf{n}\cdot\nabla I_f = c\left(\eta_f - \chi_f I_f\right),$$

for specific intensities $I_f \equiv \int_{\nu_f}^{\nu_{f+1}} I_\nu \mathrm{d}\nu$ along discrete angular unit vectors $\mathbf{n}$ defined at the volume center of each grid. When solved implicitly, the time step is not limited by the speed of light c. The emissivity $\eta_f \equiv \int_{\nu_f}^{\nu_{f+1}} \eta_\nu \mathrm{d}\nu$ and opacity $\chi_f \equiv \int_{\nu_f}^{\nu_{f+1}} \chi_\nu I_\nu \mathrm{d}\nu \,/ I_f$ are defined in the lab (fluid rest) frame, where absorption, scattering, and emission are all assumed to be isotropic. By Lorentz transformation, these source terms are re-expressed as

$$\rho\left(\kappa_{\mathrm{s},f} + \kappa_{\mathrm{a},f}\right)\left(J_{0,f} - I_{0,f}\right) + \rho\kappa_{\mathrm{p},f}\left(\varepsilon_{0,f} - J_{0,f}\right),$$

where the specific intensity $I_{0,f}$, mean radiation energy density $J_{0,f} = \int I_{0,f}\mathrm{d}\Omega_0$, and thermal emissivity $\varepsilon_{0,f} = \frac{1}{4\pi}\int_{\nu_f}^{\nu_{f+1}} B(\nu,T)\mathrm{d}\nu$ here are all defined in the comoving (radiation rest) frame, and Planck's law for spectral energy density is $B(\nu,T) = \frac{8\pi h\nu^3}{c^3}\exp\left(-\frac{h\nu}{k_\mathrm{B}T}\right)$.

The frequency domain is divided into N_f bands, where $f = 0, 1, \ldots, N_f - 1 = [0,\nu_1), [\nu_1,\nu_2), \ldots, \left[\nu_{N_f-1},\infty\right)$, and, in this context, the Planck-mean $\kappa_{\mathrm{p},f}$ and Rosseland-mean $\kappa_{\mathrm{a},f}$ absorption opacities for a given band f are defined as

$$\kappa_{\mathrm{p},f} \equiv \frac{\int_{\nu_f}^{\nu_{f+1}} \kappa_{\mathrm{a},\nu} B(\nu,T)\mathrm{d}\nu}{\int_{\nu_f}^{\nu_{f+1}} B(\nu,T)\mathrm{d}\nu},$$

$$\frac{1}{\kappa_{\mathrm{a},f}} \equiv \frac{\int_{\nu_f}^{\nu_{f+1}} \kappa_{\mathrm{a},\nu}^{-1}\frac{\partial B}{\partial T}\mathrm{d}\nu}{\int_{\nu_f}^{\nu_{f+1}} \frac{\partial B}{\partial T}\mathrm{d}\nu},$$

where we use the monochromatic absorption opacities of silicate dust grains $\kappa_{\mathrm{a},\nu}$ used by the Disk Substructures at High Angular Resolution Project (DSHARP; Birnstiel et al. 2018), with an example plotted below for four logarithmically-uniform frequency bands.

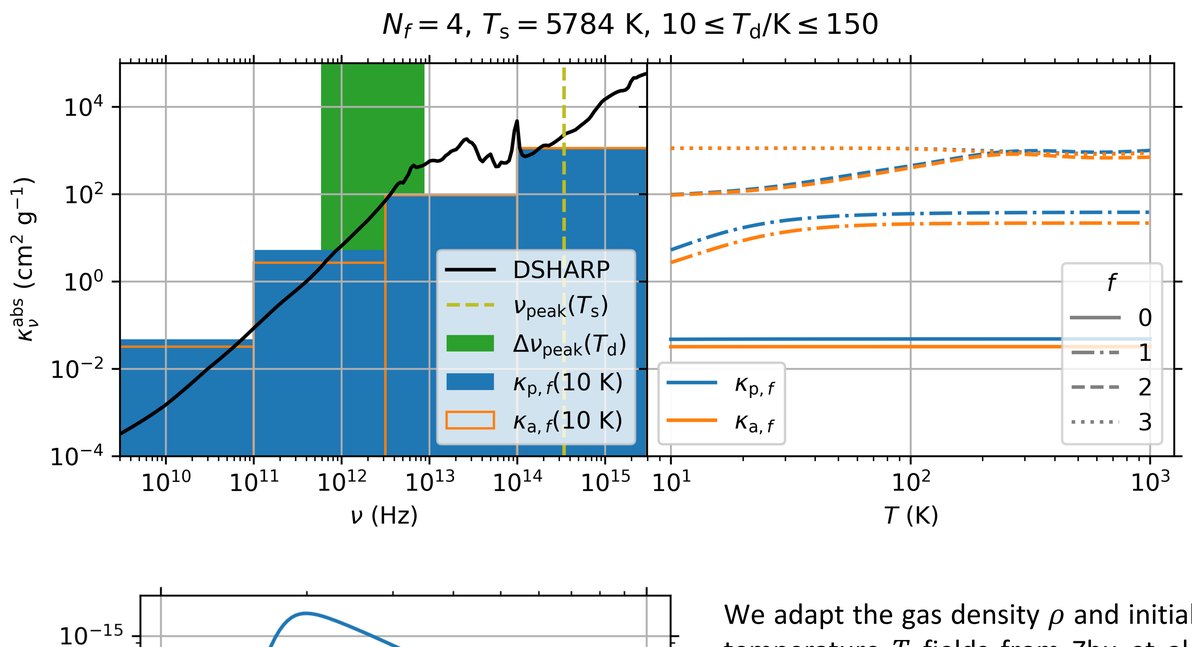

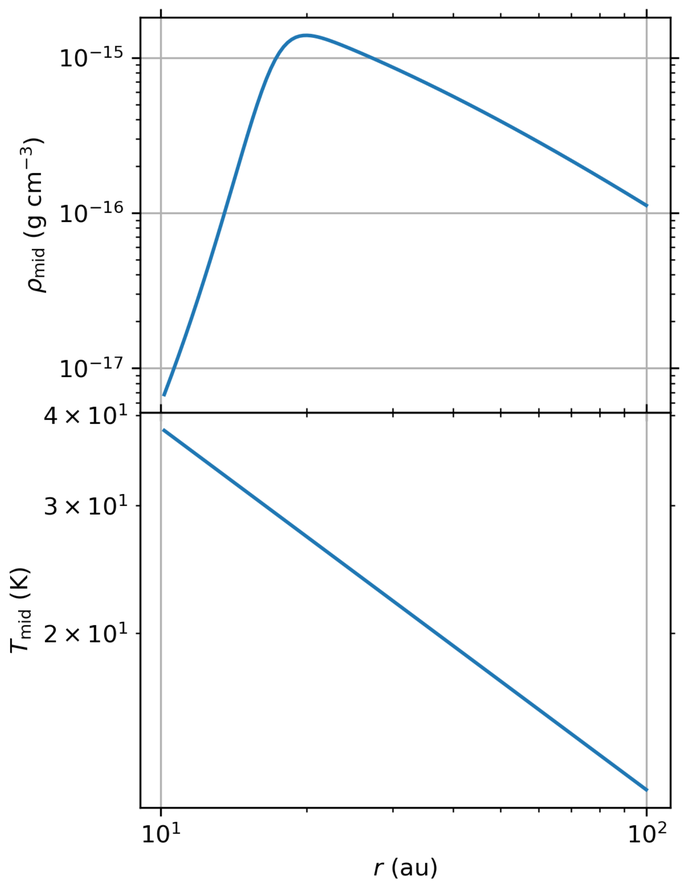

We adapt the gas density ρ and initial temperature T fields from Zhu et al. (2012) for our 2D-axisymmetric disk models which extend radially from $10\mathrm{au} < r < 100\mathrm{au}$ and $0 < \theta < \pi$ in the polar direction. With a dust-to-gas mass ratio of 1%, we assume the population of micron-sized dust grains are well coupled to the gas. As we develop and test our models, to avoid a sharp discontinuity in optical depth to stellar radiation at the inner radial boundary, we implement a sigmoid to gradually increase the disk density for $\rho(10\mathrm{au} < r < 20\mathrm{au})$. Plots to the left show the disk midplane profiles (i.e., zero latitude) of the density ρ_mid and initial temperature T_mid. The vertical structure of the disk density follows a Gaussian distribution centered on the midplane.

Results

By freezing the gas momentum and disabling radiation pressure in ATHENA++, we can better study the convergence of our models with respect to frequency resolution and compare them with our more accurate yet hydrostatic models from the Monte Carlo radiation transport code RADMC-3D. The frequency-integrated radial flux $\sum_{f=0}^{N_f-1} F_{x,f}$ and temperature snapshots below were taken once the system reached thermal equilibrium, and the white contours trace where the optical depth to stellar radiation τ_{f_s} reaches unity.

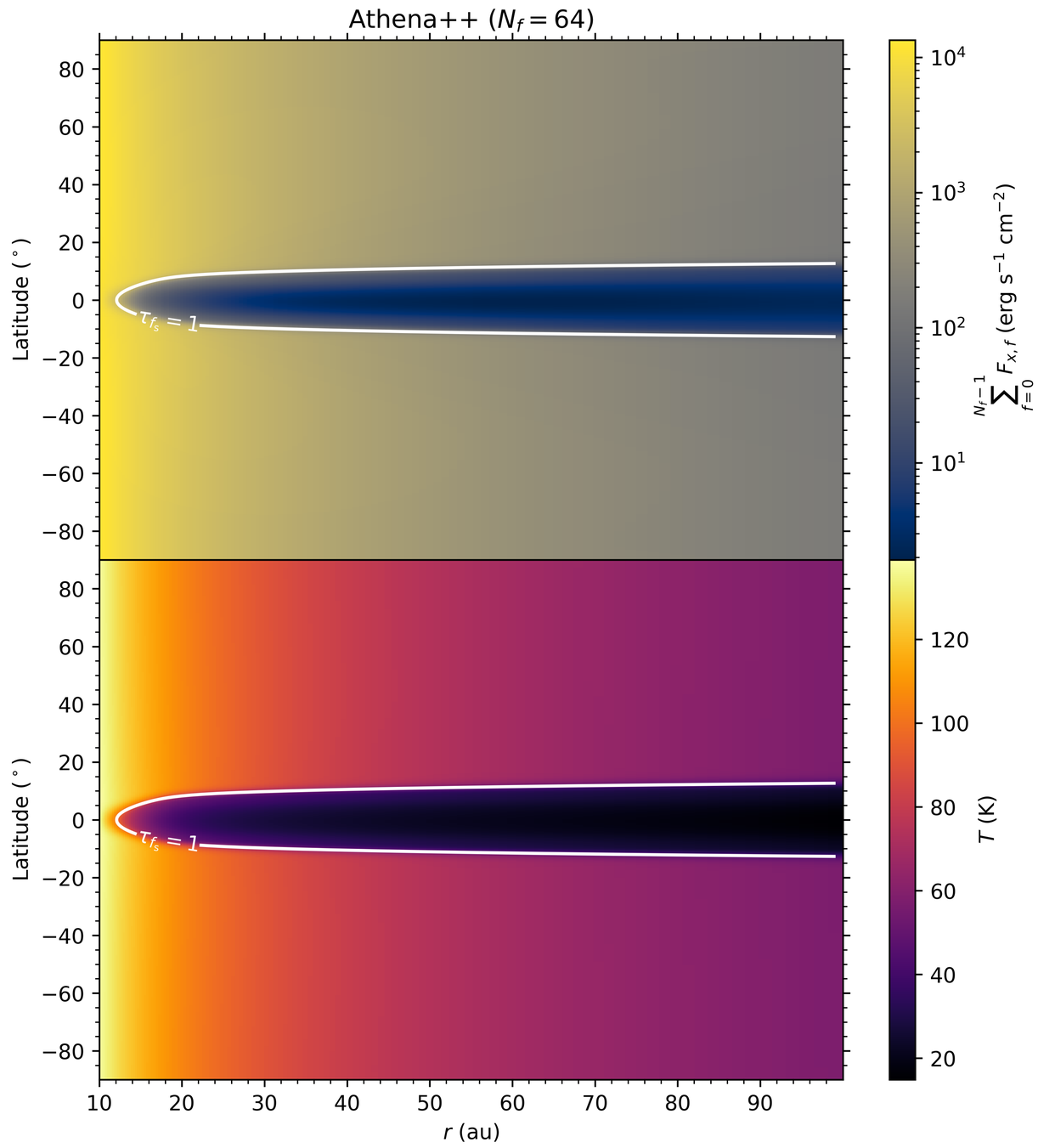

Below are radial temperature profiles along the disk midplane, atmosphere, and in between (corresponding to disk latitudes of 0°, 30°, and 5°, respectively), which help compare the results and agreement of our ATHENA++ models with those from RADMC-3D, the latter of which uses 150 frequency bands.

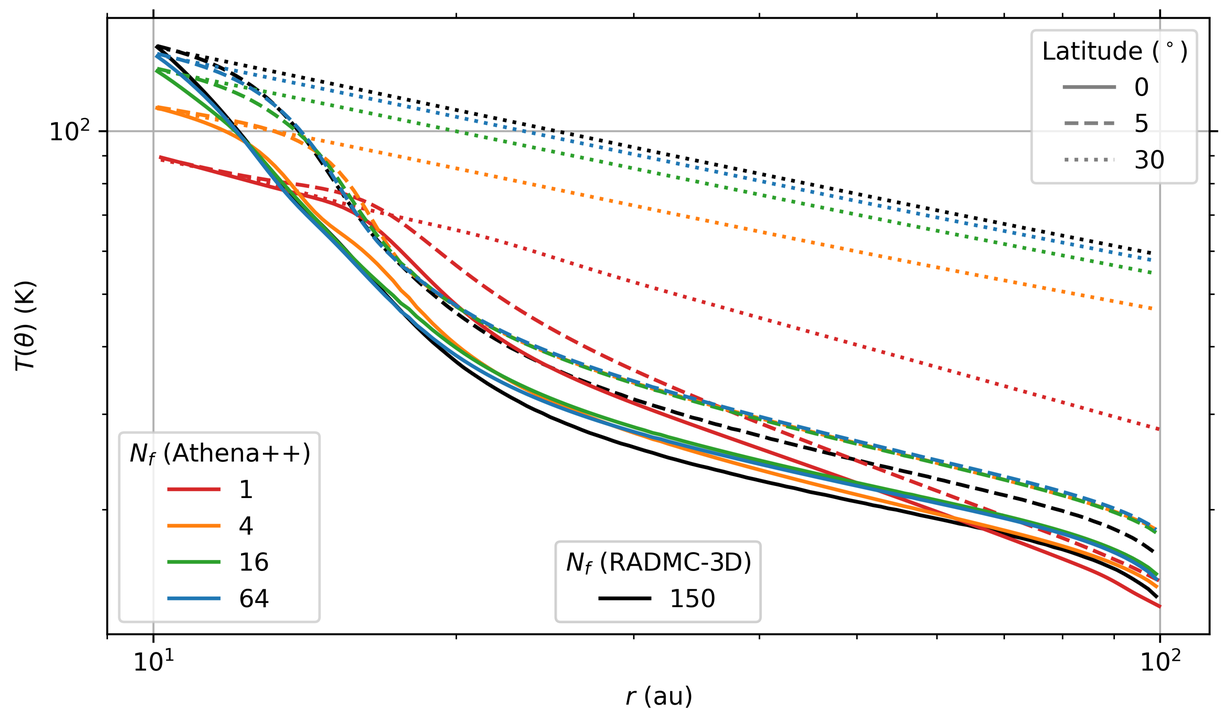

Next steps

As we have recently implemented non-uniform frequency bands in ATHENA++, we will optimize computational performance while maintaining good agreement with results from RADMC-3D. We will also add isotropic scattering opacities $\kappa_{\mathrm{s},f}$ from DSHARP to further compare with those we have already modeled in RADMC-3D. Then, with radiation hydrodynamics fully enabled in ATHENA++, we will run production models until a quasi-steady state is reached to investigate the resulting thermodynamic structure, morphology, gas kinematics, and the vertical shear instability (Nelson et al. 2013). Our framework for external sources of radiation in our disk models can also support time-dependent phenomena (e.g., stellar outbursts), which may allow us to investigate the potential for outer disk shadowing by thermally-driven surface waves in future projects.

Scan to learn more about the non-relativistic radiation transport module for ATHENA++ on the GitHub Wiki